J. Mater. Environ. Sci. 3 (6) (2012) 1045-1064
ISSN : 2528-2028
CODEN: JMESCN

Electroanalytical studies on the Interaction of 4-(N, N-Dimethylaminobenzilidine)-3-mercapto-6-methyl-1, 2, 4-triazin (4H)-5-one (DAMMT) with mild steel in perchloric acid

M. Prajila, J. Sam, J. Bincy, J. Abraham *

Department of Chemistry, University of Calicut, Calicut University P O, Kerala, India.

Received 3 June 2012, Revised 114 July 2012, Accepted 14 July 2012
* Corresponding Author: email: drabrahamj@gmail.com

Abstract

The corrosion protection properties of 4-(N, N-Dimethylaminobenzilidine)-3-mercapto-6-methyl-1, 2, 4-triazin (4H)-5-one (DAMMT) on mild steel in perchloric acid has been studied using the conventional gravimetric method, potentiodynamic polarization studies (Tafel), linear polarization studies (LPR), electrochemical impedance spectroscopy studies (EIS), adsorption studies, Scanning electron microscopy and Atomic force microscopy. The effect of inhibitor concentration, temperature, inhibition time, corrosion rate and surface characteristics are investigated. The corrosion rate and other electro analytical parameters are evaluated and the probable mechanism is also proposed. The results show that DAMMT possesses excellent corrosion inhibition property towards MS in $HClO_4$. The inhibition efficiency increases with inhibitor concentration and decreases with exposure time, temperature and acid concentration. Polarization curves show that DAMMT behave as mixed type inhibitor. Changes in the impedance parameters were indicative of the adsorption of DAMMT and formation of protective film on metal surface. The best fit for inhibitor adsorption is obtained by Langmuir isotherm model.

Key words : Corrosion inhibition, linear polarization, EIS, Electro analytical studies.

1. Introduction

Corrosion of mild steel in acid media is a challenging area which owns the attention of both academic and industrial sectors [1]. Acid solutions are widely used in the industry and the most important field of application includes acid pickling, industrial acid cleaning, acid descaling and oil and gas acidizing [2, 3]. The inhibition of corrosion in acid solutions can be well effected by variety of organic compounds and has been investigated by several workers [4-11]. The use of inhibitors is one of the most practical methods for protecting metals against corrosion in solution phase and it is becoming increasingly popular. Considerable efforts have been made to find novel and efficient corrosion inhibitors with S and / or N containing molecules [12-16].

It is established that a specific inhibitor which offer high efficiency for a particular metal in a specific media may not work with the same efficiency for other metals in the same media. The corrosion inhibition efficiency of organic molecules mainly depends on their ability to get adsorb on the metal surface with the replacement of water molecules and anions at the corroding interface [17]. The adsorption of organic molecules at the metal/solution interface is of great interest in surface

ISSN : 2528-2028
CODEN: JMESCN

science and can markedly change the corrosion resisting properties of metals. Perchloric acid and per chlorates are widely used in rocket propellant compositions which are highly corrosive to mild steel. The present study aims to understand the adsorption and inhibitive properties of 4-(N, N-dimethylaminobenzi- lidine)-3-mercapto-6-methyl-1, 2, 4-triazin (4H)-5-one (DAMMT) on mild steel in perchloric acid at different concentrations and temperatures and to establish a most probable mechanism of its protective action.

2. Experimental

2.1 *Inhibitor*

The inhibitor, DAMMT is prepared by condensing 4-amino-3-mercapto-6-methyl-1, 2, 4-triazine-4H-5-one with N, N-dimethyamine-benzaldehyde. The former compound is synthesised in the laboratory by reacting pyruvic acid with thiocarbohydrazide [18]. The purified and recrystallized DAMMT sample is characterized by physico-chemical methods. The compound is readily soluble in water at room temperature and its various concentrations were used in the present study. The structure of the compound is given in Fig.1

Structure of DAMMT

2.2 *Medium*

The medium for the study was prepared from reagent grade $HClO_4$ (E.merk) and doubly distilled water. All the tests are performed in aerated medium at different temperatures and normal atmospheric pressure.

2.3 *Materials*

The composition of the material is identified from the EDX spectrum (wt); C (0.20%), Mn (1%), P (0.03%), S (0.02%), and Fe (98.75%). The mild steel specimens used in the weight loss measurements were cut in to 4.8x1.9cm^2 coupons. The same type of coupons was used for the electrochemical studies also. But in electrochemical studies only 1cm^2 area is exposed. Before both the measurements, the samples were polished using different grade emery papers followed by washing in ethanol, acetone and finally with distilled water.

2.4 *Weight loss measurements*

The weight loss experiments were carried out in a 250 ml beaker containing test solution under total immersion conditions maintained at 30^0C. All specimens were cleaned according ASTM standard G-1-72 procedure [19-24]. After the exposure, the specimens were removed, washed initially under running tap water, to remove the loosely adhering corrosion products and finally cleaned with a mixture of 20% NaOH& 200 g/L zinc dust for 5 minutes followed by acetone. Experiments were

ISSN : 2528-2028
CODEN: JMESCN

carried out in 0.5 N, 1 N, and 2 N perchloric acid solutions with different inhibitor concentrations. From the weight loss in each experiment the corrosion rate was calculated in mills per year (mpy). In each case duplicate experiments were conducted and showed that the second results were within ± 1% of the first. Whenever the variations were very large, the data were confirmed by a third test. This inhibition efficiency was taken to represent the surface coverage (θ). The percentage inhibitive efficiency was calculated using the relation:

$$\% \text{ IE} = \frac{W_0 - W}{W_0} \times 100 \qquad (1)$$

where W_0 and W are the weight losses in the uninhibited and inhibited solutions respectively.

2.5 *Potentiodynamic polarization studies*

For the electrochemical measurements Gill AC computer controlled electrochemical workstation from ACM, UK (Model number: 1475) was used. A single wall one-compartment cell comprising a three-electrode configuration was used with platinum sheet (1 cm^2surface area) as the auxiliary electrode, saturated calomel electrode (SCE) as the reference electrode and the metal specimen as the working electrode. The working electrode was first immersed in the test solution for establishing a steady state open circuit potential prior to the electrochemical measurements. The polarization curves were obtained in the potential ranges from -250mV to +250mV with a sweep rate of 1000mV/min or16 mV/sec. The corrosion current density (*I*corr), corrosion rate (CR) and inhibition efficiency (η %) values were calculated from these curves. The inhibition efficiency (%IE) was calculated from polarization measurements using the equation;

$$\boldsymbol{\eta} = \frac{\mathbf{I_{Corr^*}} - \mathbf{I_{Corr}}}{\mathbf{I_{Corr^*}}} \times 100 \qquad (2)$$

Where $\mathbf{I_{Corr^*}}$ and $\mathbf{I_{corr}}$are uninhibited and inhibited corrosion current density respectively.

2.6 *Linear polarization method*

In order to determine the polarization resistance, Rp, the potential of the working electrode was ramped ±10mV in the vicinity of the corrosion potential at a scan rate of 1000mV/min. Polarization resistance were determined from the slope of the potential versus current lines, $\text{Rp} = \text{A} \frac{\mathbf{dE}}{\mathbf{di}}$

Where A is the surface area of the electrode. The percentage inhibition efficiency is evaluated as follows:

$$\%\text{IE} = \frac{\mathbf{Rp^* - Rp}}{\mathbf{Rp^*}} \times 100$$

Where Rp^* and Rp are the polarization resistance values in the absence and presence of the inhibitor respectively.

2.7 *Electrochemical Impedance Studies*

Impedance studies were carried out in a conventional three-electrode corrosion cell with platinum sheet (1cm^2 surface area) as auxiliary electrode, saturated calomel electrode (SCE) as the reference electrode and metal specimen as the working electrode. Electrochemical impedance spectroscopy (EIS) measurements were carried out in the frequency range of 10 KHz to 1Hz with amplitude of 10Mv (RMS) using a.c. signals at open circuit potential using Gill A C computer controlled

ISSN : 2528-2028
CODEN: JMESCN

electrochemical workstation (ACM, U.K, model no: 1475).The percentage inhibition efficiency is evaluated as follows:

$$\% \text{ IE} = \frac{\mathbf{R}_{ct} - \mathbf{R}_{ct}^{*}}{\mathbf{R}_{ct}} \times 100$$

Where $\mathbf{R}_{ct}^{*}$ and $\mathbf{R}_{ct}$ are the charge transfer resistance values in the absence and presence of the inhibitor respectively.

2.8 *Adsorption studies*

It is generally assumed that the adsorption of the inhibitor molecules on the metal surface is the essential step in the inhibition mechanism. To determine the adsorption mode, various isotherms were tested and the Langmuir isotherm found to be the best that give a straight-line graph for the plot of C/θ Vs. C. Where $\theta = U_o – U_i/U_{o;}$ U_o is the uninhibited corrosion rate, U_i is the inhibited corrosion rate and C is the concentration of the inhibitor in moles/litre.

2.9 *Scanning Electron Microscopy*

In order to have information about surface morphology of metal specimens both presence and absence of inhibitor, a Digital Microscope Imaging Scanning Electron Microscope model SU6600 (Serial No: HI-2102-0003) with an accelerating voltage of 20.0 KV is used. Samples were attached on the top of an aluminium stopper by means of carbon conductive adhesive tape. All the micrographs of the specimen were taken at a magnification of 500 SE.

2.10 *Atomic Force microscopy*

In order to establish whether inhibition is due to the formation of a film on the metal surface through adsorption, atomic force micrographs were taken. The specimens were immersed in 2N perchloric acid solution in the absence and presence of inhibitor for 24 hrs. After 24 hrs specimen were cleaned and dried at room temperature and then characterised by Atomic Force microscopy.

3. Results and discussion

3.1 *Weight loss measurements*

The weight loss enhances with increasing exposure time and increasing acid concentration and decreases with increasing inhibitor concentration at room temperature. If the concentration of inhibitor increases beyond a particular limit (threshold), the change in the inhibitive efficiency is not very significant. The corrosion rate and inhibition efficiencies were calculated using the weight loss data. The variation of corrosion rate with exposure time at various inhibitor concentrations in 0.5N, 1N and 2N perchloric acid are given in Table.1 and the corrosion inhibition efficiency with different inhibitor concentrations in mills per year (mpy) are given in Table.2. For a given concentration of the acid the corrosion rates decreases and inhibition efficiency increases considerably with the concentration of the inhibitor. However both corrosion rate and inhibition efficiency decreases with exposure time for all inhibitor concentrations. The same trend is observed for corrosion rate and inhibition efficiency with increase in the acid concentration also.

ISSN : 2528-2028
CODEN: JMESCN

Table .1 Corrosion rates (Weight loss) of MS with DAMMT in $HClO_4$solutions at 30^0C

Conc: in (ppm)	Corrosion rate (mpy) with time in Hours			
	24	48	72	96
0.5N $HClO_4$				
0	299.4	260.1	216.1	193.2
50	33.80	32.60	30.70	28.20
100	23.40	20.90	18.60	16.90
150	20.00	17.50	15.80	15.50
200	15.00	14.30	12.90	12.00
1N $HClO_4$				
0	553.1	423.8	369.5	360.0
50	67.8	63.30	56.30	55.8
100	47.60	45.30	40.70	41.60
150	72.80	70.40	73.20	69.00
200	64.40	55.00	54.40	51.60
2N $HClO_4$				
0	733.4	707.6	693.0	645.7
50	235.2	241.1	241.3	234.00
100	83.70	82.80	79.40	75.90
150	72.80	70.40	73.20	69.00
200	64.40	55.00	54.40	51.60

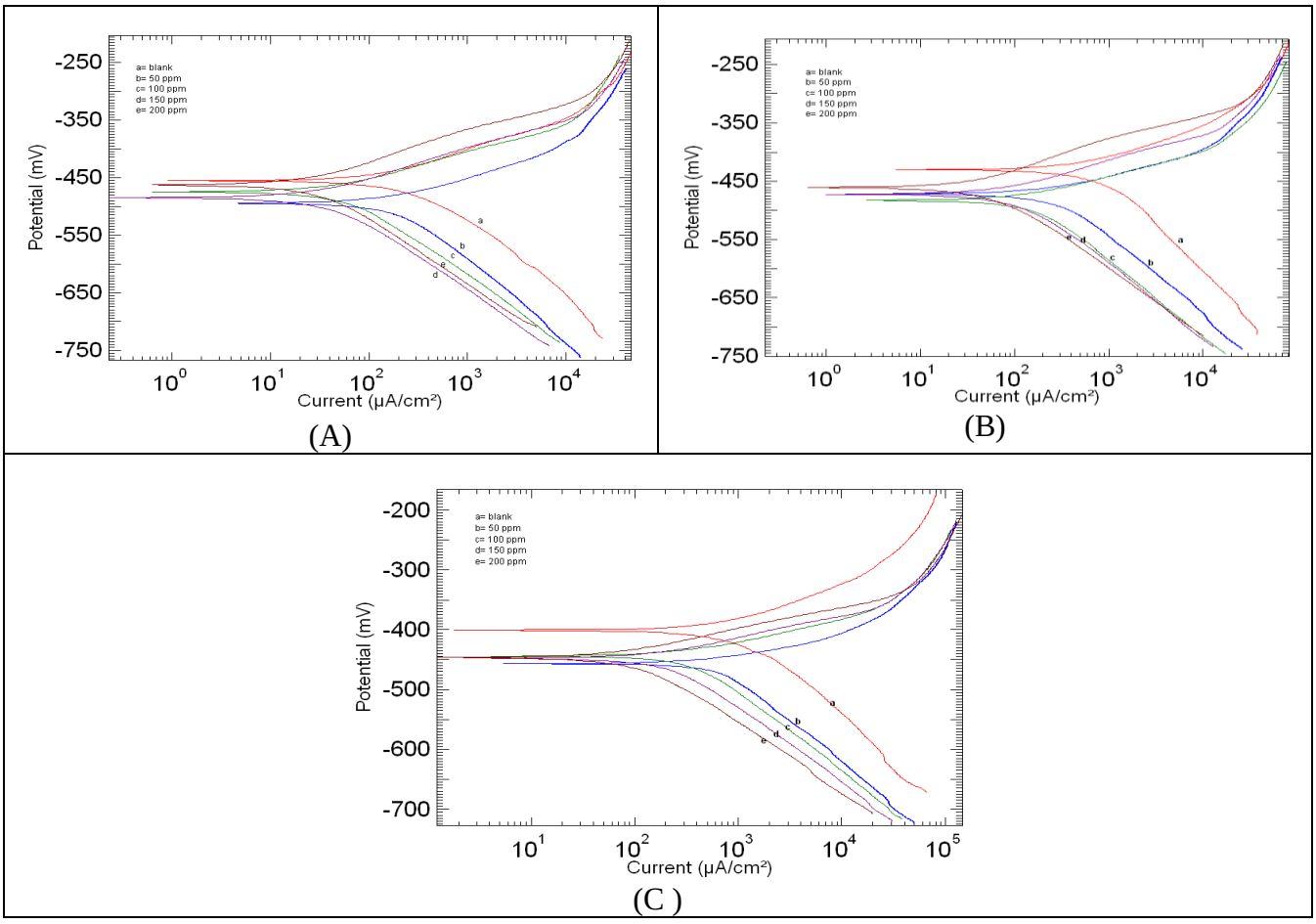

Fig.2. Anodic and cathodicTafel lines for mild steel in 0.5 N $HClO_4$ (A) 1 N $HClO_4$ (B) and 2 N $HClO_4$ (C) in the presence and absence of various concentrations of DAMMT at 30^0C.

ISSN : 2528-2028
CODEN: JMESCN

Table.2 Percentage inhibition efficiency(Weight loss) of DAMMT in $HClO_4$

Conc: in (ppm)	% Inhibition efficiency with time in Hours			
	24	48	72	96
0.5N $HClO_4$				
0	----	---	-----	-----
50	88.70	87.46	85.79	85.40
100	92.18	91.96	91.39	91.25
150	93.31	93.27	92.68	91.97
200	94.98	94.50	94.03	93.78
1N $HClO_4$				
0	----	---	-----	-----
50	87.74	85.06	84.76	84.50
100	91.39	89.31	88.98	88.44
150	92.46	92.37	92.37	91.83
200	94.86	94.24	94.28	93.86
2N $HClO_4$				
0	----	---	-----	-----
50	67.93	65.92	65.18	63.76
100	88.58	88.29	88.54	88.24
150	90.07	90.05	89.43	89.31
200	91.21	92.27	92.15	92.00

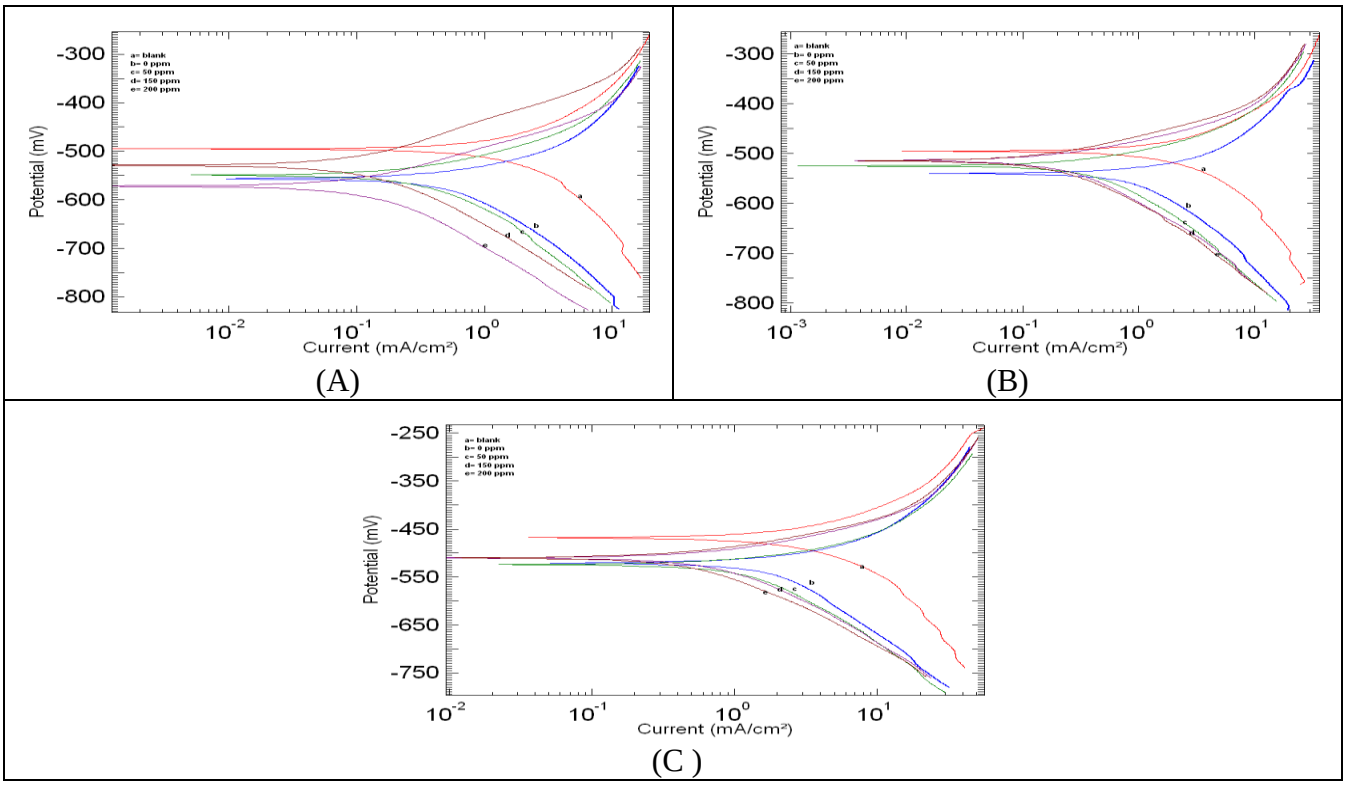

Fig.3. Anodic and cathodicTafel lines for mild steel in 0.5 N $HClO_4$ (A) 1 N $HClO_4$ (B) and 2 N $HClO_4$ (C) in the presence and absence of various concentrations of DAMMT at 40^0C

ISSN : 2528-2028
CODEN: JMESCN

3.2 *Potentiodynamic polarization studies*

Potentiodynamic polarization curves for MS in $HClO_4$ at 0.5N, 1N, and 2N solutions with various concentrations of DAMMT at temperatures 30^0C &40^0C are shown in Fig.2&3. It is clear from these figures that both the anodic metal dissolution and cathodic hydrogen evolution reactions were inhibited by DAMMT. These results suggest that DAMMT acts as mixed type corrosion inhibitor. The inhibitor molecules may first adsorb on the MS surface and blocking the available reaction sites [25]. The surface coverage increases with increase in inhibitor concentrations. The presence of defects on the metal surface permits free access to H^+ ions [26] and a significant dissolution of metal takes place, followed by desorption of the inhibitor film from the metal surface [27-29]. It is clear from these graphs that both the anodic and cathodic current values were considerably increased in uninhibited solutions compared with the inhibited ones (Fig.2&3).

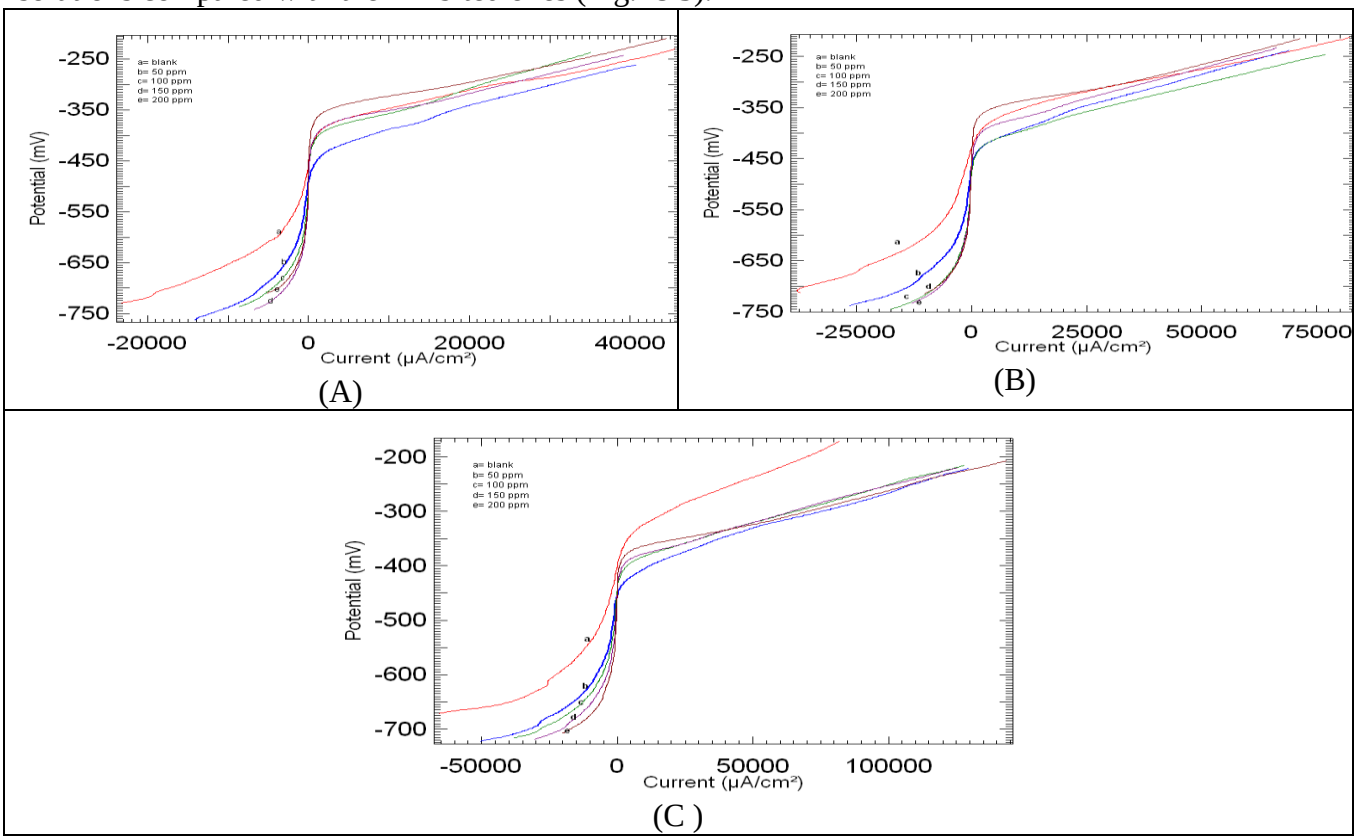

Fig.4. LPR plot for mild steel in 0.5 N $HClO_4$ (A) 1 N $HClO_4$ (B) and 2 N $HClO_4$ (C) in the presence and absence of various concentrations of DAMMT at 30^0C.

This observation can be explained with an increase in surface area of the metal due to the excess dissolution of iron. It is evident that the corrosion current density (I_{corr}) of the MS is much smaller when DAMMT is added to the aggressive solution. The change in the slope of cathodic current–potential line and anodic current–potential line indicates the modification of both anodic and cathodic reaction mechanisms in inhibited solution with time. The formation of the inhibitor film on the MS surface provides considerable protection to the metal against corrosion. The corrosion current density, inhibition efficiency and corrosion rate calculated from polarization curves at 30^0C and 40^0C are given in Table 3 & 4.

ISSN : 2528-2028
CODEN: JMESCN

Table.3 Electrochemical parameters for mild steel obtained from polarization curves in $HClO_4$ at 30^0C.

Con (ppm)	L.P.R (Ω cm^2)	β_a (mV dec^{-1})	β_c (mV dec^{-1})	C.R (mm/yr)	I corr (μA cm^{-2})	η (%P)
0.5N $HClO_4$						
Blank	10.228	62.780	96.658	18.640	0.2226	----
50	12.128	29.801	37.533	6.9010	0.0575	74.15
100	10.018	23.244	27.835	4.9031	0.0124	94.42
150	12.028	19.925	22.934	4.4667	0.0060	97.30
200	9.9068	15.289	14.888	3.8369	0.0032	98.56
1N $HClO_4$						
Blank		52.219	76.602	26.872	0.4045	-----
50	6.8137	30.359	49.130	13.877	0.1089	73.10
100	6.1324	27.758	41.280	13.638	0.0523	87.09
150	7.1952	25.469	29.110	9.5135	0.0241	94.04
200	6.0769	18.683	20.295	8.0668	0.0083	97.35
2 N $HClO_4$						
Blank	5.3892	61.652	83.376	33.141	0.5931	----
50	3.3536	26.049	32.476	21.719	0.2367	60.09
100	3.7035	20.413	28.405	16.160	0.0961	83.79
150	3.7254	19.768	27.335	15.517	0.0487	91.78
200	2.9356	16.527	18.813	15.122	0.0157	97.35

Table.4 AC impedance data of mild steel with DAMMT in $HClO_4$solutions at 30^0C

Con (ppm)	-Ecorr (mV)	Rct (Ω cm^2)	Rsol (Ω cm^2)	Cdl (μF cm^{-2})	I corr (μA cm^{-2})	C.R (mm/yr)	η (%P)
0.5N $HClO_4$							
Blank	481	29.62	3.556	7.683	0.8807	10.207	---
50	498	104.1	3.331	4.832	0.2505	2.9043	71.73
100	483	332.3	2.990	3.915	0.0784	0.9098	91.08
150	494	457.8	2.812	3.157	0.0569	0.6604	93.62
200	457	575.3	2.678	3.308	0.0453	0.5256	94.85
1N $HClO_4$							
Blank	456	12.34	2.249	11.11	2.1140	24.5010	---
50	485	40.30	1.892	6.168	0.6473	7.5024	69.37
100	495	103.80	1.781	4.753	0.2513	2.9127	88.11
150	466	166.2	1.738	3.911	0.1569	1.8191	92.57
200	459	299.1	1.701	3.723	0.0872	1.0108	95.87
2N $HClO_4$							
Blank	421	10.69	1.199	25.98	2.4403	28.283	---
50	467	16.12	1.134	11.14	1.6182	18.756	33.68
100	469	32.59	1.120	8.346	0.8005	9.2773	67.19
150	464	54.41	1.062	5.811	0.4795	5.5568	80.35
200	452	133.00	0.9635	5.013	0.1961	2.2732	91.96

ISSN : 2528-2028
CODEN: JMESCN

3.4 *Electrochemical impedance spectroscopy*

The performance of the organic coatings on the metal surface can be evaluated from the EIS studies and this has been widely used for the investigation of the protective properties of organic inhibitor molecules on metals. It does not disturb the double layer at the metal/solution interface and therefore, more reliable results can be obtained from this technique [30, 31]. The Nyquist plots for the MS in different concentrations of $HClO_4$ solutions with various concentrations of DAMMT after 1 h of immersion at temperatures 30^0C &40^0C are shown in Fig. 4&5 and the representative Bode diagrams are given in Fig.6&7. It is clear from these figures that in uninhibited solution, Nyquist plot yields slightly depressed semi circles and only one time constant in Bode format.

This indicates the corrosion of the MS in the absence of inhibitor which is mainly controlled by a charge transfer process [28, 29,32]. In the evaluation of Nyquist plots, the difference in real impedance at lower and higher frequencies is commonly considered as a charge transfer resistance.

Table.5 ΔG_{ads} (KJ mol^{-1}) and $_{Kads}$(mol^{-1}) at 30^0C.

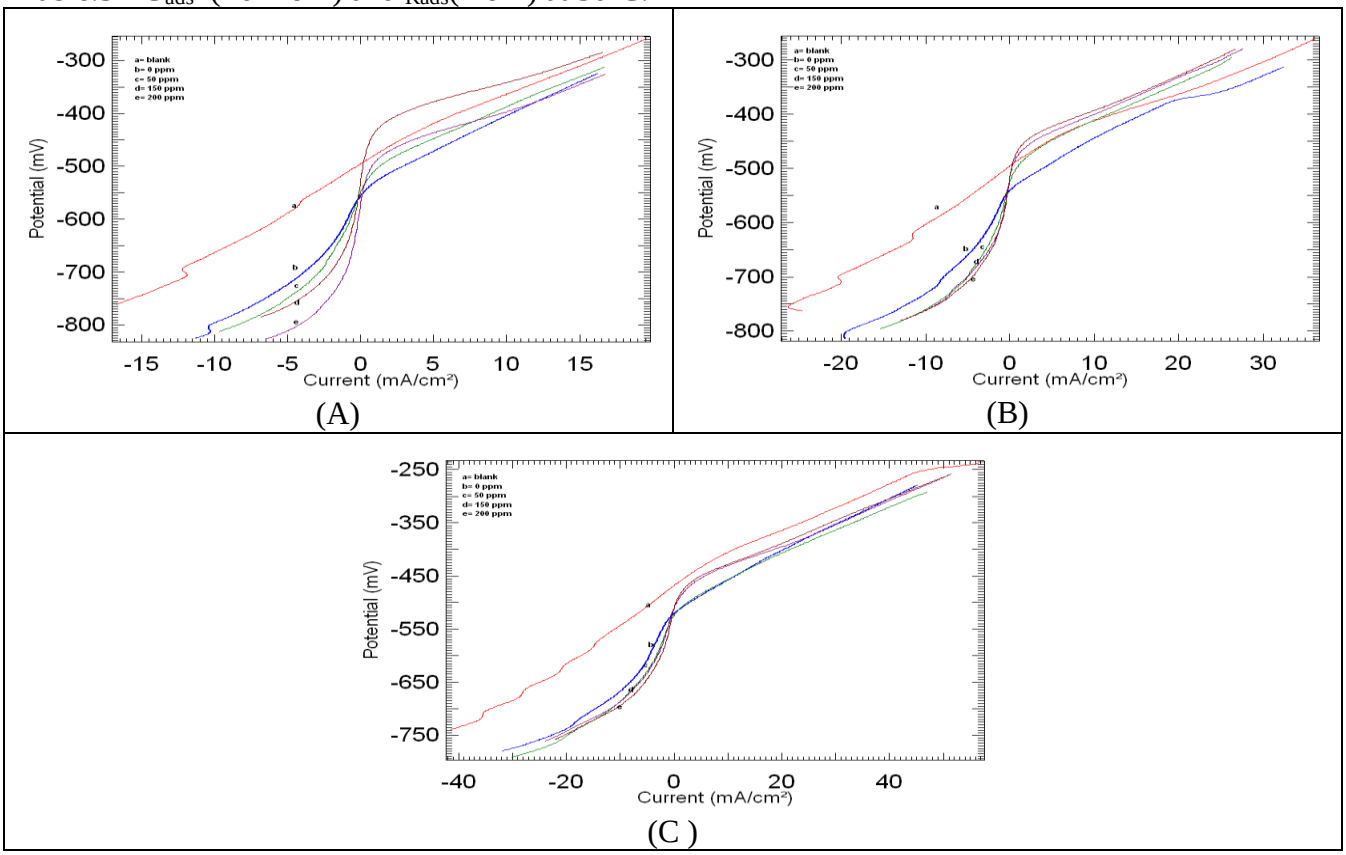

Fig.5. LPR plot for mild steel in 0.5 N $HClO_4$ (A) 1 N $HClO_4$ (B) and 2 N $HClO_4$ (C) in the presence and absence of various concentrations of DAMMT at 40^0C.

The charge transfer resistance must be corresponding to the resistance between the metal and OHP (Outer Helmholtz Plane). The contribution of all resistances corresponding to the metal/solution interface like charge transfer resistance (*R*ct), diffuse layer resistance (*R*d), accumulation resistance (*R*a), film resistance (*R*f), etc. must be taken into account. Therefore, in this study, the difference in real impedance at lower and higher frequencies is considered as the polarization resistance (*R*p) [28-33]. The addition of DAMMT to the acid solution leads to a change in the impedance diagrams both in shape and size, with a depressed semicircle at the higher frequency part of the spectrum.

ISSN : 2528-2028
CODEN: JMESCN

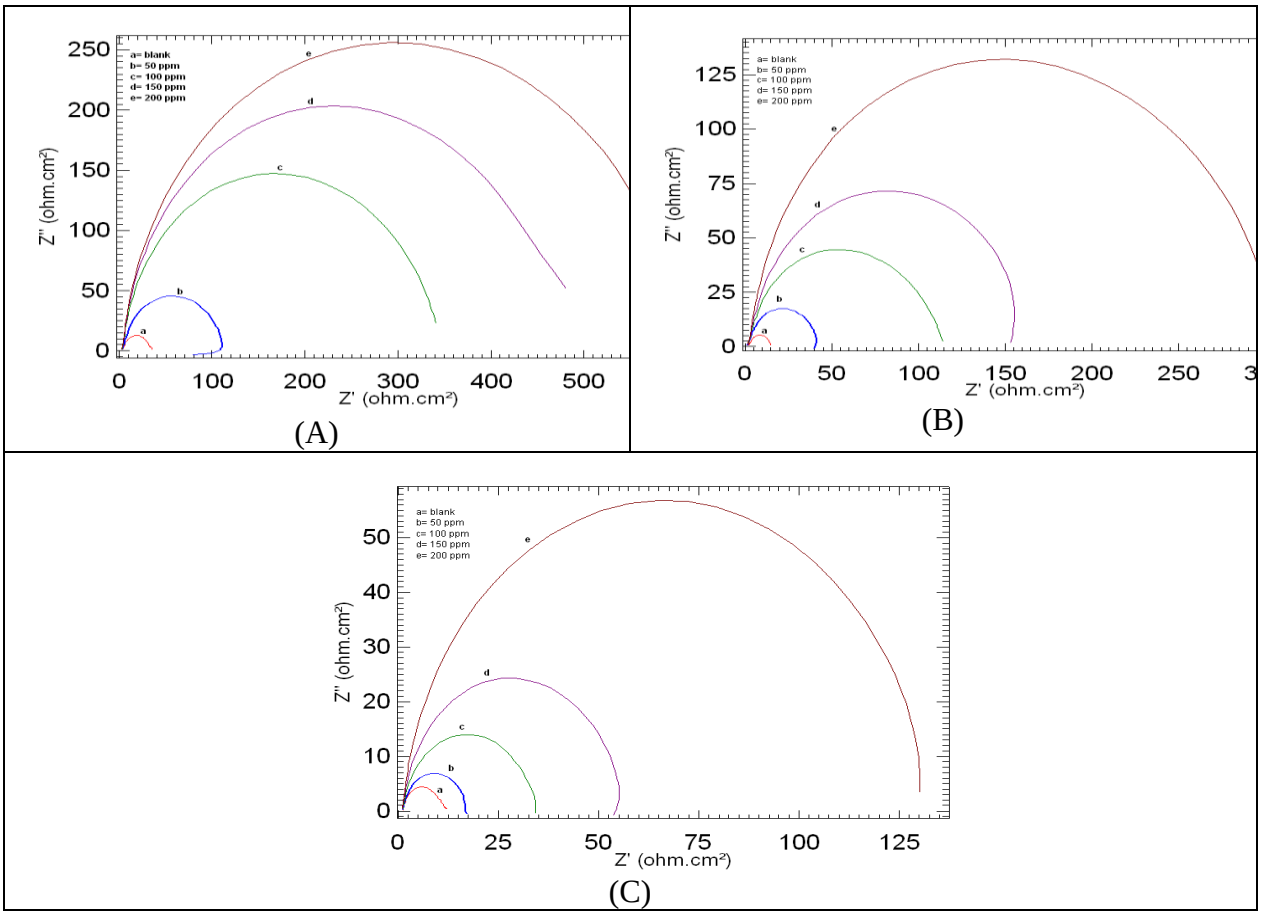

Fig.6. Nyquist plot for mild steel in 0.5 N $HClO_4$ (A) 1 N $HClO_4$ (B) and 2 N $HClO_4$ (C) in the presence and absence of various concentrations of DAMMT at 30^0C.

In this case, the MS corrosion takes place only on the free surface of the metal and/or within the pores due to diffusion of dissolved oxygen through these pores of the protective layer [33]. The %IE values obtained from the EIS are comparable and run parallel with those obtained from the potentiodynamic polarization measurements. The EIS results at 30^0C and 40^0C are summarized in table 5&6

Table.5 ΔG_{ads} (KJ mol^{-1}) and $_{Kads}$(mol^{-1}) at 30^0C

Conc (ppm)	0.5 N $HClO_4$		1 N $HClO_4$		2 N $HClO_4$	
	ΔG_{ads}	K_{ads}	ΔG_{ads}	K_{ads}	ΔG_{ads}	K_{ads}
50	-33.95	14665	-33.66	13090	29.93	2935
100	-35.69	29509	-34.89	21416	31.68	5918
150	-35.60	28462	-35.17	24004	32.39	7878
200	-35.43	26613	-36.01	33542	34.24	16527

Straight lines were obtained in the potential range and the parallel increase in the corrosion inhibition efficiency for MS in $HClO_4$ with increasing inhibitor concentration can be explained on the basis of inhibitor adsorption on MS.

ISSN : 2528-2028
CODEN: JMESCN

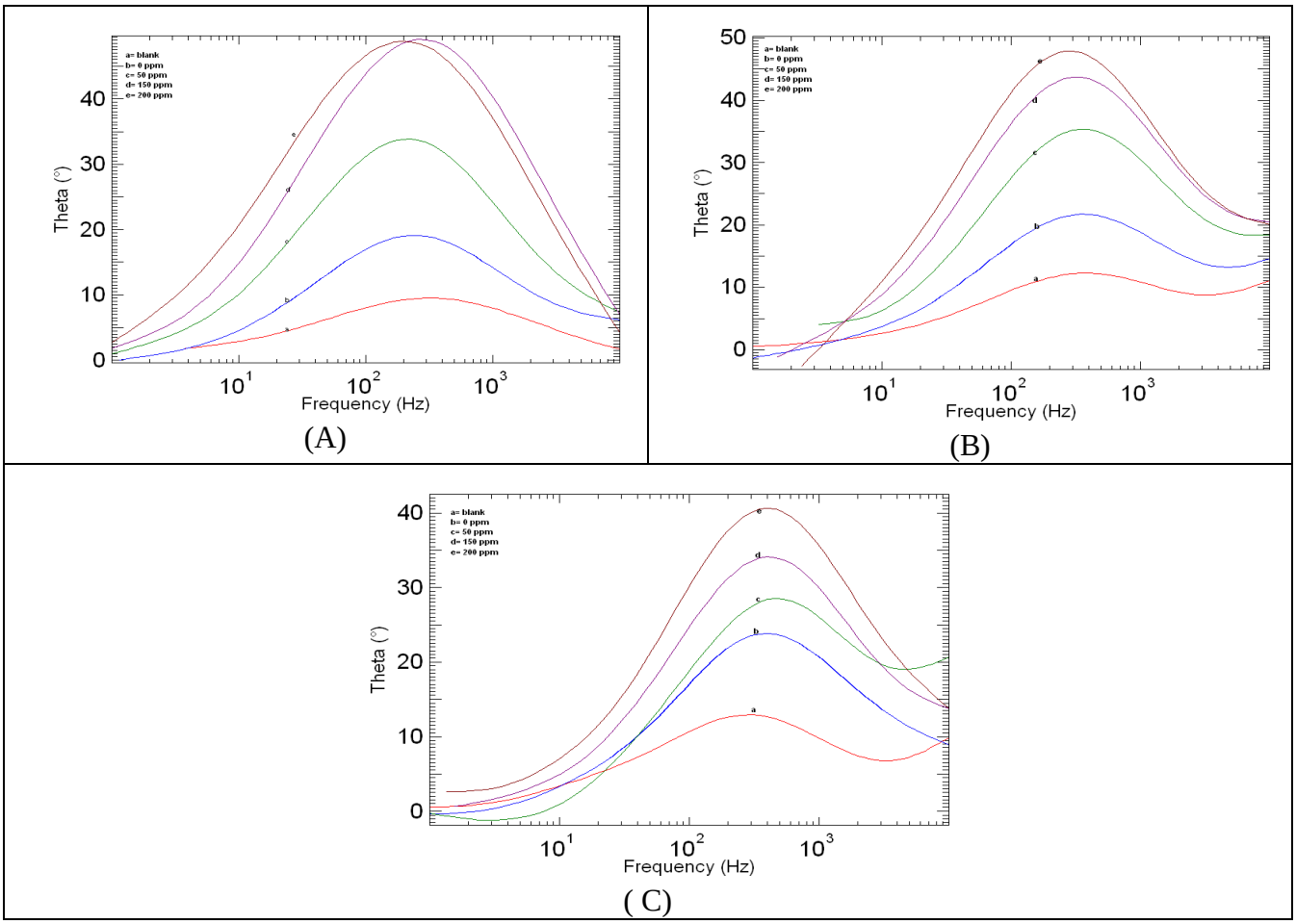

Fig.7. Bode-phase plot for mild steel in 0.5 N $HClO_4$ (A) 1 N $HClO_4$ (B) and 2 N $HClO_4$ (C) in the presence and absence of various concentrations of DAMMT at 40^0C.

3.4 *Linear polarization studies*

Polarization resistance values were obtained from the slope of the polarization curves in the potential range of ±10mV with respect to the corrosion potential at a sweep rate of 1000mV/min. Generally, the Rp values increases with increasing inhibitor concentrations as seen in Fig.8&9**.** The rest potential values were used to calculate the inhibition efficiency.

Table.6 Electrochemical parameters for mild steel obtained from polarization curves in $HClO_4$ at 40^0C

Conc.	L.P.R	β_a	β_c	C.R	I corr	η
(ppm)	(Ω cm^2)	(mV dec^{-1})	(mV dec^{-1})	(mm/yr)	(μA cm^{-2})	(%P)
0.5N HCLO4						
Blank	14.98	109.57	119.62	19.23	1.09	.....
50	21.33	58.55	108.55	8.99	0.34	68.00
100	24.24	56.67	86.09	7.10	0.19	82.00
150	26.14	56.14	67.40	5.90	0.06	94.00
200	31.25	55.86	56.53	4.53	0.05	95.33
1N HCLO4						

ISSN : 2528-2028
CODEN: JMESCN

Blank	8.43	113.52	138.10	37.24	1.89	
50	12.40	53.08	132.06	15.38	0.75	60.48
100	15.24	52.71	105.31	11.62	0.30	84.00
150	15.20	48.71	89.50	10.46	0.17	91.08
200	15.59	47.70	71.88	9.27	0.10	94.52
2N HCLO4						
Blank	6.08	117.77	139.70	52.95	2.87	----
50	7.78	60.77	135.75	27.19	1.35	53.02
100	8.20	51.89	116.84	22.08	0.83	70.90
150	7.65	49.63	94.83	21.46	0.44	84.70
200	7.78	42.21	79.76	17.89	0.27	90.50

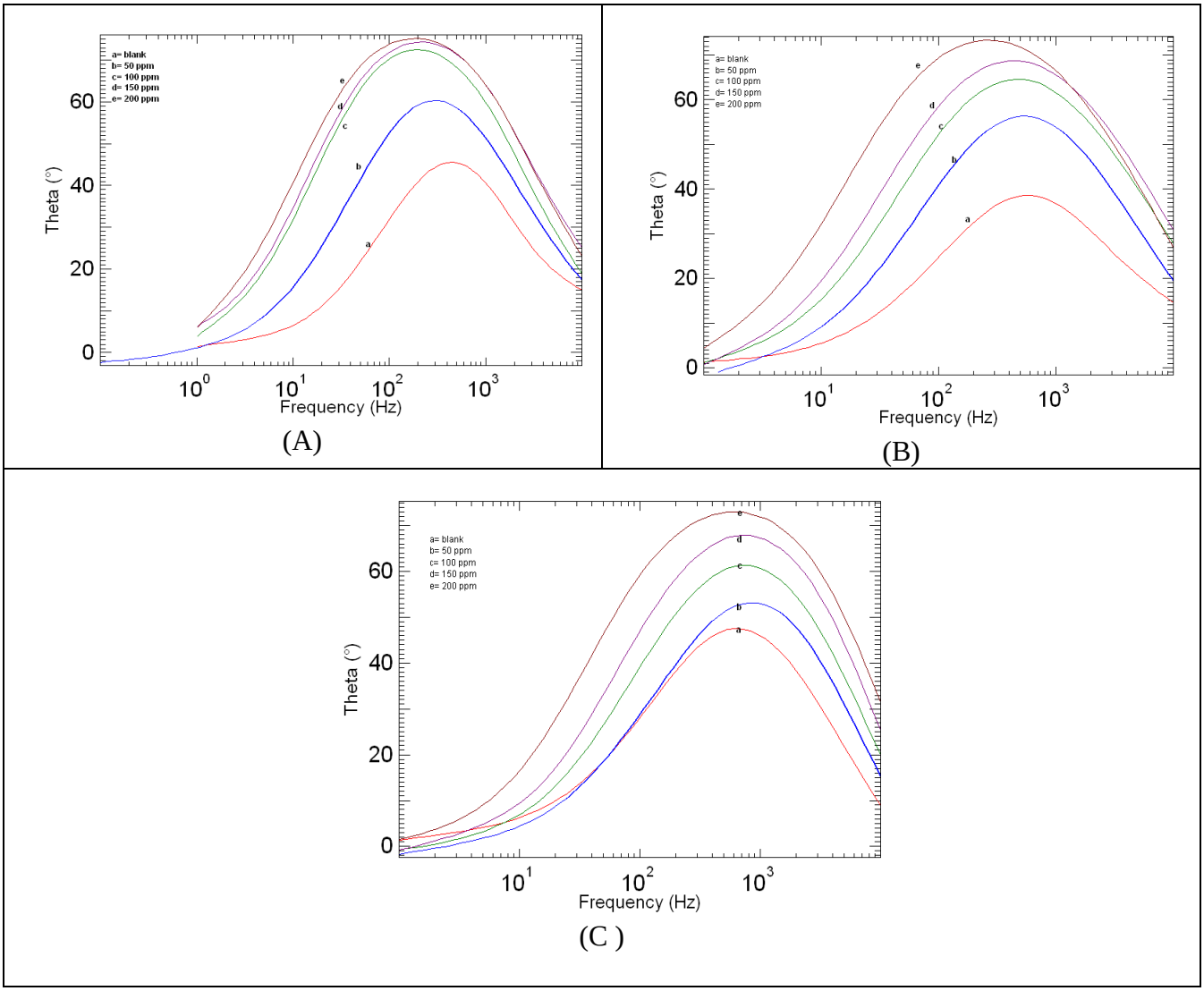

Fig.8. Bode phase plot for mild steel in 0.5 N $HClO_4$ (A) 1 N $HClO_4$ (B) and 2 N $HClO_4$ (C) in the presence and absence of various concentrations of DAMMT at 30^0C.

ISSN : 2528-2028
CODEN: JMESCN

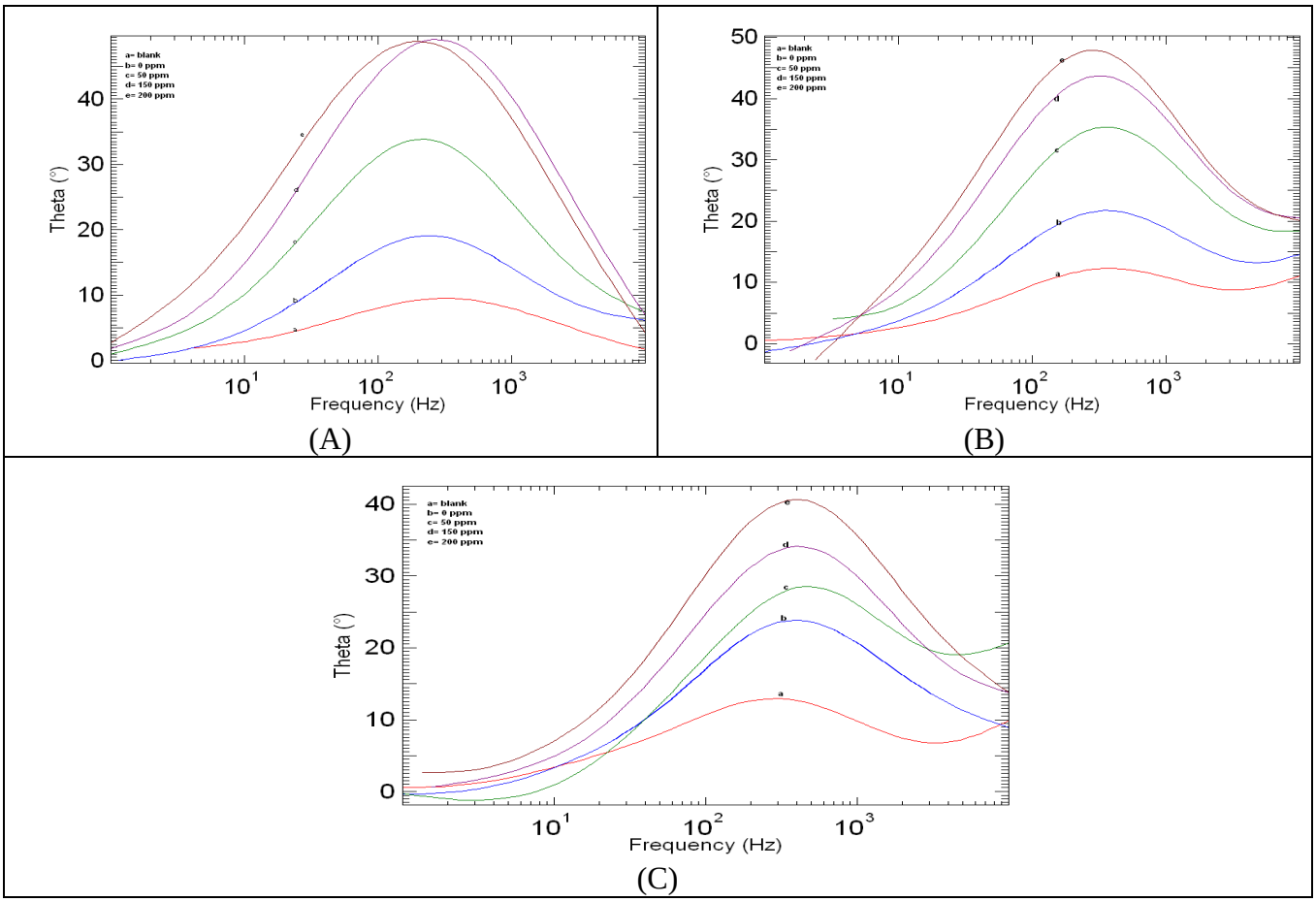

Fig.9. Bode-phase plot for mild steel in 0.5 N $HClO_4$ (A) 1 N $HClO_4$ (B) and 2 N $HClO_4$ (C) in the presence and absence of various concentrations of DAMMT at 40^0C.

3.5*Adsorption studies*

Adsorption plays a prominent role in the inhibition of metallic corrosion by organic molecules. Many investigators have used Langmuir adsorption isotherm to study inhibitor characteristics assuming that the inhibitors adsorbed on the metal surface decrease the surface area available for electrode reactions to take place[34-38]. The values of surface coverage (θ) related to different concentrations of DAMMT in 0.5N,1N&2N $HClO_4$ solutions obtained from Tafel polarization or EIS measurements have been used to explain the best isotherm to determine adsorption process. The adsorption of organic corrosion inhibitor at metal-solution interface is a substitutional adsorption process between organic molecules and the metallic surface. In the concentration range studied, the best correlation between experimental result and isotherm functions are obtained using Langmuir adsorption isotherm. The Langmuir adsorption isotherm for monolayer adsorption [39] is given by $\theta/1-\theta = KC_{inhi}$

On rearranging,

$$C_{inhi}/\theta = 1/K + C_{inhi}$$

Where $\theta = U_o - U_i/U_o$; $U_o$is the uninhibited corrosion rate, U_i is the inhibited corrosion rate, C_{inhi} is the concentration of the inhibitor in moles/litre and K is the equilibrium constant for the adsorption process.

ISSN : 2528-2028
CODEN: JMESCN

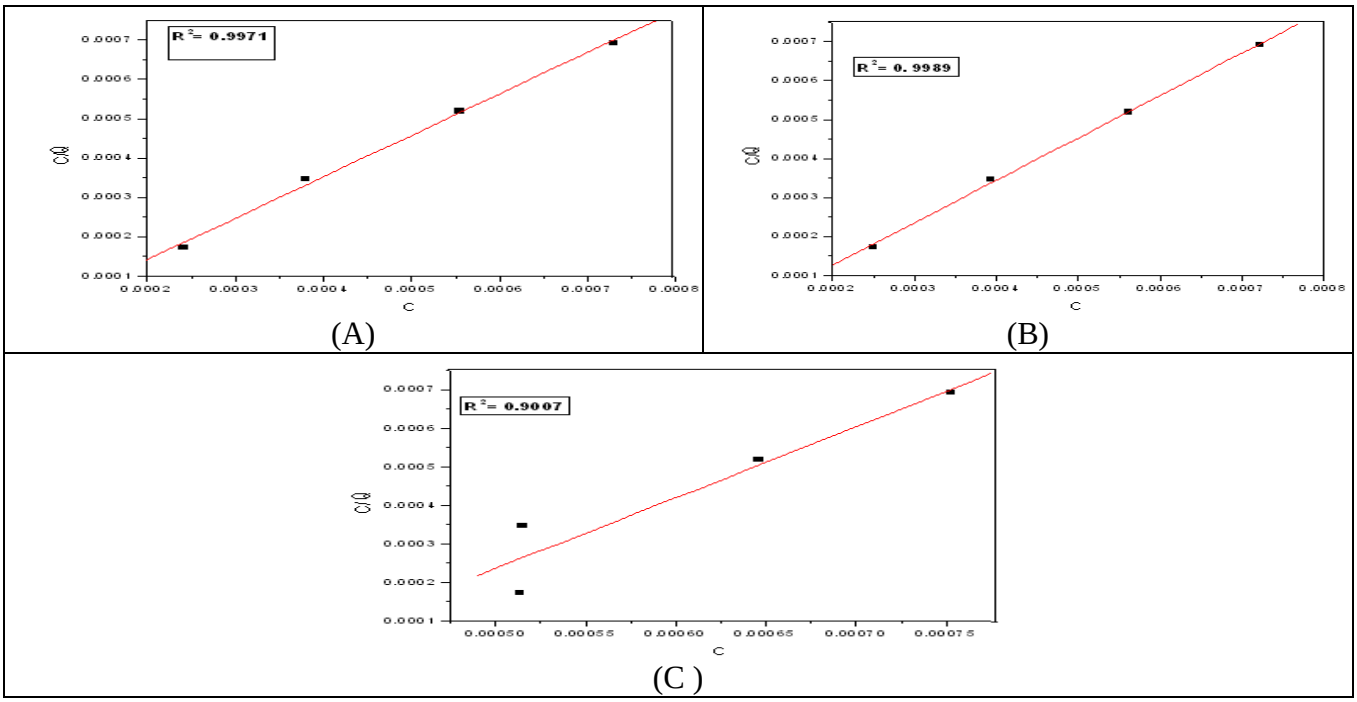

Fig.10. The Langmuir adsorption isotherm for mild steel in 0.5 N $HClO_4$ (A) 1 N $HClO_4$ (B) and 2 N $HClO_4$ (C) in the presence and absence of various concentrations of DAMMT at 30^0C.

The plots at the experimental temperature (300K) corresponding to mild steel is a straight line, but the gradients are not equal to unity as is expected for the ideal Langmuir adsorption isotherm (Fig.10&11). This may be due to the interaction of adsorbed molecules on the metal surface, which is completely ignored during the derivation of Langmuir equation.

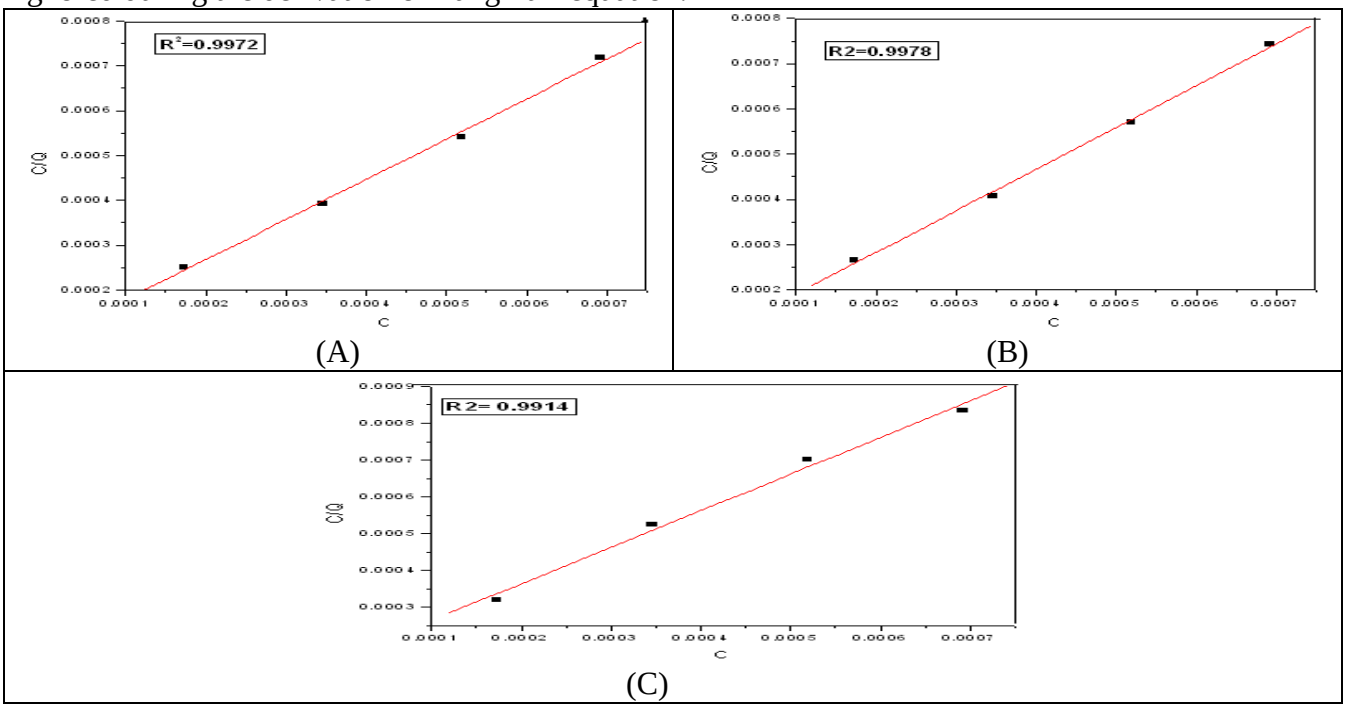

Fig.11. The Langmuir adsorption isotherm for mild steel in 0.5 N $HClO_4$ (A) 1 N $HClO_4$ (B) and 2 N $HClO_4$ (C) in the presence and absence of various concentrations of DAMMT at 40^0C.

ISSN : 2528-2028
CODEN: JMESCN

Organic molecules having polar atoms or groups being adsorbed on the metal surface may interact by mutual attraction or repulsion. These interactions would affect the heat of adsorption of the inhibitor molecules. If the interaction is repulsive, the heat of adsorption will be negative and if it is attractive, the heat of adsorption will be positive. The probable mechanism of cathodic hydrogen evolution reaction may be given as :

$$Fe + H^+ \leftrightarrow [FeH^+]_{ads}$$
$$[FeH^+]_{ads} + e^- \rightarrow [FeH]_{ads}$$
$$[FeH]_{ads} + H^+ + e^- \rightarrow Fe + H_2$$

The protonated DAMMT molecules are adsorbed at cathodic sites in competition with hydrogen ions that going to reduce to H_2 gas [37]. The free energy of adsorption ΔG_{ads} is calculated using the equation, $\Delta \mathbf{G_{ads}} = -\mathbf{RT}\ln[55.5\boldsymbol{\theta}/\mathbf{C}(1-\boldsymbol{\theta})]$.Where C is the concentration of the inhibitor expressed in ppm. Negative value of ΔG_{ads} ensures the spontaneity of adsorption process and stability of adsorbed layer on the mild steel surface. If the value of ΔG_{ads} is around -20 kJ/mol or lower then the adsorption phenomenon is considered as physisorption, and if the value is around -40 kJ/mol or higher is considered as chemisorptions [40]. The values of K and ΔG_{ads} for different inhibitor concentrations at 30^0C and 40^0C are given in Tables 7&8 and the results indicate that adsorption involves both physisorption and chemisorption.

Table.7 AC impedance data of mild steel with DAMMT in $HClO_4$solutions at 40^0C

Conc.	-Ecorr	Rct	Rsol	Cdl	I corr	C.R	η
(ppm)	(mV)	(Ω cm^2)	(Ω cm^2)	(μF cm^{-2})	(μA cm^{-2})	(mm/yr)	(%P)
0.5N HClO4							
Blank	505	5.71	10.34	38.87	4.57	52.95	---
50	570	19.02	11.19	17.82	1.37	15.90	69.00
100	557	50.02	10.08	7.87	0.53	6.14	88.00
150	575	147.30	8.63	5.73	0.18	2.05	96.00
200	531	155.8	8.14	8.56	0.17	1.94	96.33
1N HClO4							
Blank	510	4.48	5.98	26.51	5.83	67.55	----
50	560	12.76	5.96	21.03	2.04	23.69	64.92
100	546	30.01	5.89	7.24	0.87	10.07	85.00
150	535	53.52	5.41	6.22	0.49	5.65	91.00
200	535	66.13	5.20	6.10	0.39	4.57	93.23
2N HClO4							
Blank	481	4.21	4.09	105.00	6.20	71.28	---
50	540	9.23	3.61	24.38	2.83	32.75	54.00
100	527	12.57	3.02	23.91	2.08	24.05	66.50
150	511	16.26	3.72	13.20	1.60	18.59	74.10
200	509	24.28	3.59	9.73	1.05	12.15	83.07

ISSN : 2528-2028
CODEN: JMESCN

Table.8 ΔG_{ads} (KJ mol^{-1}) and K_{ads} (mol^{-1}) at 40^0 C

Conc(ppm)	0.5 N $HClO_4$		1 N $HClO_4$		2 N $HClO_4$	
	ΔG_{ads}	K_{ads}	ΔG_{ads}	K_{ads}	ΔG_{ads}	K_{ads}
50	-35.07	12865	-34.59	10696	-33.41	6785
100	-36.37	21194	-35.70	16377	-32.91	5610
150	-38.40	46242	-36.15	19481	-32.85	5483
200	-37.88	37930	-36.11	19199	-33.51	7055

Table.9 The value of activation parameters, Ea, ΔH^0_a, ΔS^0_a for mild steel mild steel with different concentrations of DAMMT in $HClO_4$solutions.

Conc	Ea	ΔH^0_a	ΔS^0_a
0.5N $HClO_4$			
Blank	124	121.99	156.46
50	128	125.96	159.13
100	144	141.98	202.27
150	87	84.58	10.22
200	99	97.49	50.96
1N $HClO_4$			
Blank	76	74.21	6.06
50	86	84.30	29.51
100	93	91.40	45.06
150	86	83.61	15.46
200	113	110.75	100.18
2N $HClO_4$			
Blank	70	68.01	-13.21
50	42	39.79	-109.74
100	72	69.68	-16.96
150	91	88.61	41.23
200	126	124.21	151.31

3.7*Scanning Electron Microscopy*

Surface morphology of mild steel is examined by using SEM. Scanning Electron Microscopy of polished Mild Steel surface, Mild Steel surface in 2N $HClO_4$ in the absence and presence of inhibitor after 24 hr exposure is shown in fig. 12.

From the SEM images it is clear that the mild steel surface is strongly damaged in the absence of inhibitor. But in the presence of inhibitors surface damage is reduced to a greater extend. So it can be concluded that the corrosion of mild steel in perchloric acid is strongly inhibited in the presence of DAMMT.

ISSN : 2528-2028
CODEN: JMESCN

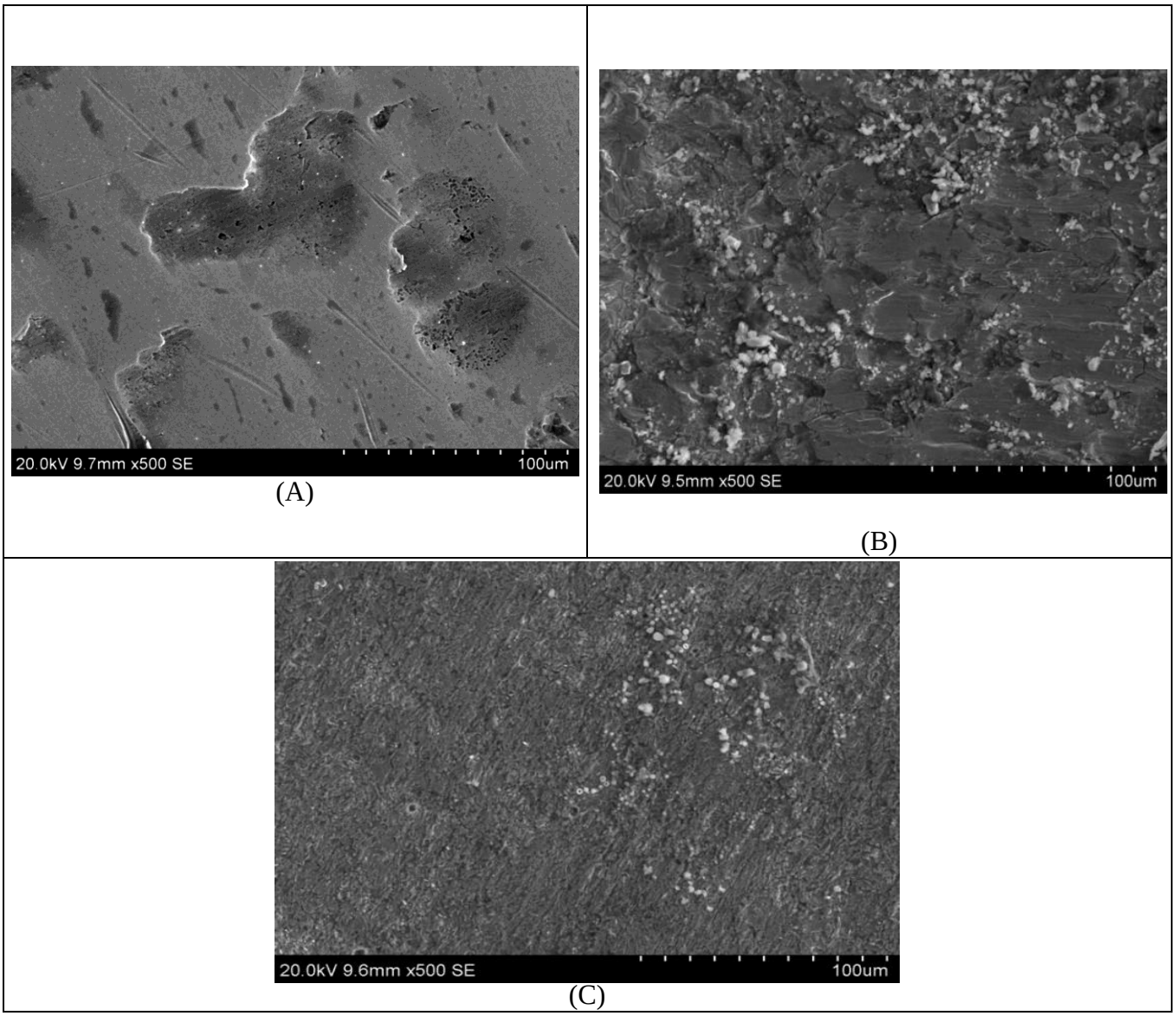

Fig. 12. SEM images of (A)polished mild steel surface(B) mild steel surface exposed in 2N $HClO_4$ solution and (C) mild steel surface exposed in 2N $HClO_4$ solution with DAMMT.

3.8 *Atomic Force microscopy*

Atomic Force microscopic observations were done for polished Mild Steel surface, Mild Steel surface in 2N $HClO_4$ in the absence and presence of inhibitor after 24 hr exposure and are presented in Fig. 13. The roughness factor obtained from Fig. 13 A, B, & C are 7.588, 129.810, and 52.206 nm respectively. It indicates that the presence of inhibitor reduces the roughness of the surface by adsorbing on the metal surface.

ISSN : 2528-2028
CODEN: JMESCN

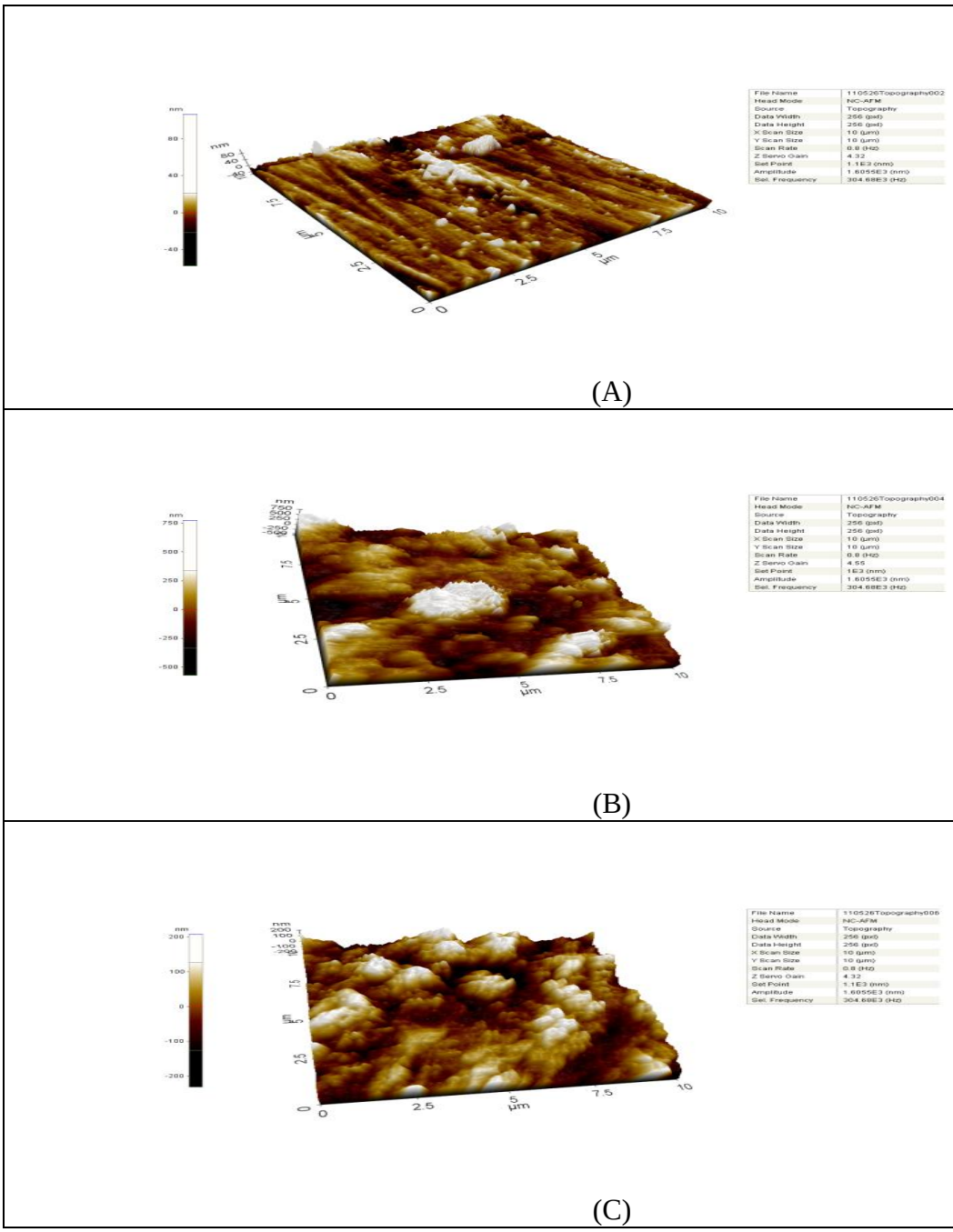

AFM images of (A) polished mild steel surface(B) mild steel surface exposed in 2N $HClO_4$ solution and (C) mild steel surface exposed in 2N $HClO_4$ solution with DAMMT.

4. Conclusion

- DAMMT shows high inhibition efficiency towards mild steel corrosion in different concentrations of perchloric acid.
- The percentage inhibition efficiency increases with increase in inhibitor concentration and decreases with increase in acid concentration and exposure periods.

ISSN : 2528-2028
CODEN: JMESCN

- The inhibitor molecules adsorb on the MS surface and blocking the reaction sites. The surface area available for the attack of the corrosive species decreases with increasing inhibitor concentrations.
- A higher coverage of the inhibitor molecules on the metal surface was obtained in solutions with higher inhibitor concentrations.
- The best fit for inhibitor adsorption is obtained by Langmuir isotherm model.
- The values of ΔG_{ads} for different inhibitor concentrations indicate that adsorption involves both physisorption and chemisorption.
- Results of polarisation studies suggest that the inhibitor, DAMMT, acts as mixed type inhibitor.

Acknowledgement The authors are grateful to Kerala State Council for Science Technology and Environment (KSCSTE) for financial support in the form of a major research project 018/SRSPS/2006/CSTE.

References

1. Bentiss, F., Traisnel, M., Lagrenee, M. *Corros. Sci*. 42 (2000) 127.
2. Schmitt, G.*Br. Corros. J*. 19 (1984) 165.
3. Mernari, B., Traisnel, M., Bentiss, F., Lagrenee, M.*Corros. Sci.* 40 (1998) 391.
4. Otero, E., Bastida, J M. *Mater. Corros*. 47 (1992) 133.
5. Batros, M., Hakerman, M. *J. Electrochem. Soc*. 139 (1992)3429
6. Hashi, I., Zucchi, F., in Proceedings of the seventh European Symposium on Corrosion inhibitors (7SEIC), Ann. University, Ferrara, NS, Sez. V, Vol.9, 1990, p.321
7. Kutej, P., Vosta, J., Pancir, J., Macak, J., Hakerman, N. *J. Electrochem. Soc.* 142 (1995) 829
8. Szklarska-Smialowska, Z., Kaminski, M. *Corros. Sci*. 13 (1973) 1.
9. Uhrea, J., Aramaki, K. *J. Electrochem. Soc,* 138 (1991) 3245
10. Kertit, S., Hammouti, B. *Appl. Surf. Sci*. 93 (1996) 59.
11. Bentiss, F., Lagrenee, M., Traisnel, M., Mernari, B., El Attari, H. *J. Appl. Electrochem.* 29 (1999) 1073.
12. Keles, H., Keles, M.¸ Dehri, I., Serindag, O.,Colloids Surf. A: Physicochem. Eng. Aspects. 320 (2008) 138.
13. Tang, L., Li, X, Li L, Mu., Liu, G.Mater. Chem. Phys. 97 (2006) 301.
14. Solmaz, R., Kardas, G., Yazıcı, B., Erbil, B.*Prot. Met.* 43 (2007) 476.
15. Popova, A., Sokolova, E., Raicheva, S.,Christov, M.*Corros. Sci.* 45 (2003) 33.
16. Kardas, G., Solmaz, R.*Corros. Rev.* 24 (2006) 151.
17. Bockris, J O M., Reddy, A K N., Modern Electrochemistry, vol. 2,Plenum Publishing Corporation, 227West 17th, Street, New York, 1976.
18.Sam John., Bincy Joseph., Aravindakshan K K., Abraham Joseph.*Mater. Chem. Phys.* 122 (2010) 374
19. Bag, S K., Chakraborty, S B., Chaudhari, S R. *J. Indian Chem. Soc*, 70 (1993) 24.
20. Ailor, W H., Hand book of corrosion testing and evaluation, John Wiley and Sons, New York (1971).
21. Talati, J D., Modi, R M.*Br. Corros. J* 10 (1975) 103.
22. Talati, J D., Patel, G A.*Br. Corros. J*, 11 (1976) 47.
23. Champion, F A., Corrosion testing procedure, 2nd Ed. Chapman and Hall, London (1964).
24. Fontana, M G., Greene, N D. Corrosion engineering, McGraw Hill (1984).

ISSN : 2528-2028
CODEN: JMESCN

25. Fuchs-Godec, R., Colloids Surf. A: Physicochem. Eng. Aspects 280 (2006) 130.
26. Chetouani, A., Hammouti, B., Benhadda, T., Daoudi, M.*App. Surf. Sci.*249 (2005) 375.
27. El Mehdi, B., Mernari, B., Traisnel, M., Bentiss, F., Lagrenee, M. *Mater. Chem. Phys.*77 (2002) 489.
28. El Achouri, M., Kertit, S., Gouttaya, H M., Nciri, B., Bensouda, Y., Perez, L., Infante, M R., Elkacemi, K.*Prog. Org. Coat.* 43 (2001) 267.
29. Lorenz, W J., Mansfeld, F.*Corros. Sci.* 31 (1986) 467.
30. Erbil, M.*Chim. Acta Turcica* 1 (1988) 59.
31. Dehri, I., So¨zu¨ sag˘lam H., Erbil, M.*Prog. Org. Coat.* 48 (2003) 118.
32. Chetouani, A., Aouniti, A., Hammouti, B., Benchat, N., Benhadda, T., Kertit, S. *Corros. Sci.* 45 (2003) 1675.
33. Tuken, T., Yazıcı, B., Erbil, M.*Mater. Chem. Phys.* 99 (2006) 459.
34. Allen, C F H., Edens, C O., Van, J Allen J. *Org- Syn. Coll* 3, 394.
35. Hoar, T P., Holliday, R D. *J. Appl. Chem,* 3 (1953) 502.
36. Hora, T P., Khera, R P. Proc. Eru. Symp. Corros Inhibitors, Ferrara (1960) 73.
37. Solmaz, R., Kardas, G., Culha, M., Yazici, B., Erbil, M. *Electrochimica Acta.* 53 (2008) 5941.
38. Kaan, E C., Akay, A A., Atakol, O. *Mater.Chem.Phy.* 93 (2005)325.
39. Agarwal, R., Namboodhiri, T K G. *Corros Sci*. 30 (1990) 37
40. Bincy J., Sam J., Abraham J., Narayana B., *Indian J. Chem. Tech.* 17 (2010) 366

(2012); http://www.jmaterenvironsci.com